

Sulfido-Bridged Tetranuclear Titanium–Iridium Complexes with an Unconventional Tetrahedral Iridium Center

Miguel A. Casado, Miguel A. Ciriano,* Andrew J. Edwards, Fernando J. Lahoz, Luis A. Oro,* and Jesús J. Pérez-Torrente

Departamento de Química Inorgánica, ICMA, Facultad de Ciencias, Universidad de Zaragoza-CSIC, E-50009 Zaragoza, Spain

Received March 4, 1999

A general route to the complexes $[\text{CpTi}(\mu_3\text{-S})_3\text{M}_3(\text{diolefin})_3]$ ($\text{M} = \text{Rh}$, diolefin = cod, nbd, tffb; $\text{M} = \text{Ir}$, diolefin = cod) consists of the reactions of the anion $[\text{Cp}_2\text{Ti}_2(\mu\text{-S})_2(\text{S})_2]^{2-}$, obtained by mono-deprotonation of $\text{Cp}_2\text{Ti}(\text{SH})_2$ with butyllithium in THF, with the appropriate complexes $[\{\text{M}(\mu\text{-Cl})(\text{diolefin})\}_2]$. Replacement of the diolefin by carbon monoxide in $[\text{CpTi}(\mu_3\text{-S})_3\text{M}_3(\text{diolefin})_3]$ gives the carbonyl derivatives $[\text{CpTi}(\mu_3\text{-S})_3\text{M}_3(\text{CO})_6]$. Further reactions of the carbonyliridium complex with tertiary phosphine and phosphite ligands produce the 62-e valence clusters $[\text{CpTi}(\mu_3\text{-S})_3\text{Ir}_3(\mu\text{-CO})(\text{CO})_3(\text{PR}_3)_3]$ ($\text{PR}_3 = \text{PPh}_3, \text{PMe}_3, \text{P}(\text{OMe})_3, \text{PMePh}_2$). Remarkable features in the structure of these compounds, as found for $[\text{CpTi}(\mu_3\text{-S})_3\text{Ir}_3(\mu\text{-CO})(\text{CO})_3(\text{P}(\text{OMe})_3)_3]$ by X-ray diffraction studies, are a distorted tetrahedral metal framework with short Ir–Ir distances and a tetrahedral coordination of the iridium atom closest to the titanium. A delocalized bonding scheme can be proposed for the iridium triangle and, at least, an interaction between the tetrahedral iridium and the titanium atom. The complexes $[\text{CpTi}(\mu_3\text{-S})_3\text{Ir}_3(\mu\text{-CO})(\text{CO})_3(\text{PR}_3)_3]$ quickly exchange all their carbonyl ligands with ^{13}CO under normal conditions to give the labeled complexes. Indeed, an equilibrium between the compounds $[\text{CpTi}(\mu_3\text{-S})_3\text{Ir}_3(\mu\text{-}^{13}\text{CO})(^{13}\text{CO})_3(\text{PR}_3)_3]$ and $[\text{CpTi}(\mu_3\text{-S})_3\text{Ir}_3(\mu\text{-}^{13}\text{CO})(^{13}\text{CO})_4(\text{PR}_3)_2]$ and free phosphine exists under an atmosphere of ^{13}CO . In addition, these compounds are fluxional, since they exhibit a single carbonyl resonance in the low-temperature $^{13}\text{C}\{^1\text{H}\}$ NMR spectrum, probably due to very fast carbonyl scrambling. Furthermore, the reaction of $[\text{CpTi}(\mu_3\text{-S})_3\text{Ir}_3(\mu\text{-CO})(\text{CO})_3(\text{PPh}_3)_3]$ with HBF_4 gives the unsymmetric and nonfluxional hydride of formula $[\text{CpTi}(\mu_3\text{-S})_3\text{Ir}_3(\mu\text{-CO})(\text{H})(\text{CO})_3(\text{PPh}_3)_3]\text{BF}_4$.

Introduction

Complexes having two widely divergent metals, one a Lewis-acid early transition metal and the other an electron-rich late transition metal (early–late heterobimetallics, ELHB) are promising candidates for new stoichiometric and catalytic reactions,¹ and they could serve as models for studying the role of the support in heterogeneously catalyzed reactions.² Properties such as multifunctionality and cooperative effects have been predicted if the metal centers can “communicate” with one another. Nevertheless, the problems found to meet the different coordination environments of both metals in close proximity could be as great as the expectations, and thus synthetic strategies leading to new complexes are highly desirable.¹

Transition metal complexes with bridging sulfido ligands have a broad scope ranging from widely studied biological systems and applied industrial processes, such as dehydrodesulfurization and catalysis, to novel chemistry of molecular systems.^{3,4} Although a variety of tetrathiometalates have been very effective in preparing mixed-metal complexes,⁵ organometallic early–late metal

complexes are relatively uncommon, and efforts to develop this chemistry have been reported recently.⁶ We have previously reported the formation of unusual early–late titanium–rhodium complexes with incomplete cubane structures⁷ starting from $\text{Cp}_2\text{Ti}(\text{SH})_2$ and some unexpected oxosulfido titanium–rhodium clusters with an incomplete doubly fused cubane structure.⁸

Results and Discussion

Syntheses and Characterization of the Tetranuclear Complexes $[\text{CpTi}(\mu_3\text{-S})_3\{\text{M}(\text{diolefin})\}_3]$ ($\text{M} = \text{Rh}, \text{Ir}$). The reported reactivity of $\text{Cp}_2\text{Ti}(\text{SH})_2$ has

(4) For recent references, see: (a) Firth, A. V.; Witt, E.; Stephan, D. W. *Organometallics* **1998**, *17*, 3716. (b) Nishioka, T.; Isobe, K.; Kinoshita, I.; Ozawa, Y.; Vazquez de Miguel, A.; Nakai, T.; Miyajama, S. *Organometallics* **1998**, *17*, 1637. (c) Shiu, K. B.; Wang, S. L.; Liao, F. L.; Chiang, M. Y.; Peng, S. M.; Lee, G. H.; Wang, J. C.; Liou, L. S. *Organometallics* **1998**, *17*, 1790. (d) Nishio, M.; Matsuzaka, H.; Mizobe, Y.; Hidai, M. *J. Organomet. Chem.* **1997**, *263*, 119.

(5) For recent references see: (a) Yuki, M.; Okazaki, M.; Inomata, S.; Ogino, H. *Angew. Chem., Int. Ed. Engl.* **1998**, *37*, 2126. (b) Howard, K. E.; Rauchfuss, T. B.; Wilson, S. R. *Inorg. Chem.* **1988**, *27*, 3561.

(6) For recent references see: (a) Stang, P. J.; Persky, N. E. *J. Chem. Soc., Chem. Commun.* **1997**, *77*. (b) Desmurs, P.; Visseaux, M.; Baudry, D.; Dormond, A.; Nief, F.; Ricard, L. *Organometallics* **1996**, *15*, 4718. (c) Dick, D. G.; Hou, Z.; Stephan, D. W. *Organometallics* **1992**, *11*, 2378.

(7) Atencio, R.; Casado, M. A.; Ciriano, M. A.; Lahoz, F. J.; Pérez-Torrente, J. J.; Tiripicchio, A.; Oro, L. A.; *J. Organomet. Chem.* **1996**, *514*, 103.

(8) Casado, M. A.; Ciriano, M. A.; Edwards, A. J.; Lahoz, F. J.; Pérez-Torrente, J. J.; Oro, L. A. *Organometallics* **1998**, *17*, 3414.

(1) Stephan, D. G. *Coord. Chem. Rev.* **1989**, *95*, 41.

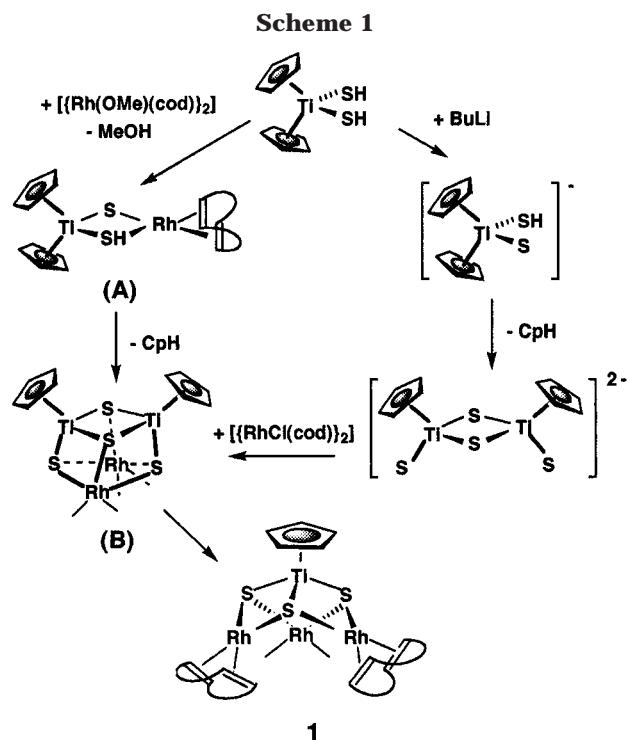
(2) Herrmann, W. A.; Cornils, B. *Angew. Chem., Int. Ed. Engl.* **1997**, *36*, 1049.

(3) Stiefel, E. I.; Matsumoto, K. *Transition Metal Sulfur Chemistry, Biological and Industrial Significance*, ACS Symposium Series 653; American Chemical Society: Washington, DC, 1996.

been very limited ever since its preparation in 1965.⁹ In particular, the acidity of the hydrosulfido ligand is unknown. A previous report from this laboratory indicates the ability of $\text{Cp}_2\text{Ti}(\text{SH})_2$ to protonate the methoxo ligand in $[\{\text{Rh}(\mu\text{-Ome})(\text{tfbb})\}_2]$, yielding the heterotetranuclear complex $[\text{CpTi}(\mu_3\text{-S})_3\{\text{Rh}(\text{tfbb})\}_3]$ (tfbb = tetrafluorobenzobarrelene).⁷ The analogous complex $[\text{CpTi}(\mu_3\text{-S})_3\{\text{Rh}(\text{cod})\}_3]$ (**1**) results from the reaction of $\text{Cp}_2\text{Ti}(\text{SH})_2$ with $[\{\text{Rh}(\mu\text{-Ome})(\text{cod})\}_2]$ (cod = 1,5-cyclooctadiene) under strictly anhydrous conditions in THF.⁸ Complex **1** is an orange solid which crystallizes from the reaction medium. Yields are moderate and do not increase substantially upon varying the molar ratio of the starting materials. Monitoring the reaction by ^1H NMR spectroscopy confirms that it proceeds quickly with formation of the main product **1**, along with methanol, free cyclopentadiene, and uncharacterized cyclopentadienyl titanium complexes. Attempts to separate these compounds from the mother liquor by column chromatography resulted only in a slight increase in the yield of the main compound **1**.

A similar protocol using $\text{Cp}_2\text{Ti}(\text{SH})_2$ and $[\{\text{Ir}(\mu\text{-Ome})(\text{cod})\}_2]$ is not suitable for the synthesis of the analogous Ti–Ir complex $[\text{CpTi}(\mu_3\text{-S})_3\{\text{Ir}(\text{cod})\}_3]$. This reaction follows an alternative pathway resulting in the formation of the known cluster¹⁰ $[\text{Ir}_3(\mu_3\text{-S})_2(\mu\text{-H})(\text{cod})_3]$ in high yield. As the hydrido-iridium cluster can be obtained from $[\{\text{Ir}(\mu\text{-Cl})(\text{cod})\}_2]$ and NaHS or H_2S , the titanium complex acts as a source of hydrosulfido ligands for iridium, one of which produces the oxidative-addition of the S–H bond leading to the hydrido ligand. To avoid this undesired reaction, a deprotonated form of $\text{Cp}_2\text{Ti}(\text{SH})_2$ would be more appropriate for the synthesis of iridium–titanium complexes. With this aim, $\text{Cp}_2\text{Ti}(\text{SH})_2$ was reacted with butyllithium in THF. Brown insoluble solids are obtained on mixing these compounds in a 1:2 molar ratio, while a beautiful green solution containing free cyclopentadiene and the anionic complex $[\text{Cp}_2\text{Ti}_2(\mu\text{-S})_2(\text{S})_2]^{2-}$ results from a 1:1 molar ratio. The complex $\text{Na}_2[\text{Cp}_2\text{Ti}_2(\mu\text{-S})_2(\text{S})_2]$, showing a color and ^1H NMR spectrum identical to the aforementioned green solution, has been isolated recently by Kubas¹¹ from the deprotonation of $\text{Cp}_2\text{Ti}(\text{SH})_2$ with sodium hydride.

The green solution of the anion $[\text{Cp}_2\text{Ti}_2(\mu\text{-S})_2(\text{S})_2]^{2-}$, prepared in situ, is an excellent starting material for the synthesis of heterometallic iridium–titanium and rhodium–titanium complexes with sulfido bridging ligands and thus provides insight on the reactions mentioned above. Reactions of $[\text{Cp}_2\text{Ti}_2(\mu\text{-S})_2(\text{S})_2]^{2-}$ with the chlorocomplexes $[\{\text{M}(\mu\text{-Cl})(\text{diolefin})\}_2]$ give the compounds $[\text{CpTi}(\mu_3\text{-S})_3\{\text{M}(\text{diolefin})\}_3]$ (M = Rh, diolefin = cod (**1**), nbd (**2**), tfbb; Ir, diolefin = cod (**3**)). Complexes **1–3** are isolated as air-stable crystalline solids in moderate yields (60–65%) and show the molecular ions corresponding to the proposed formulas in their mass spectra. Although **1–3** show some kind of nonrigidity in solution, since the proton and carbon olefin resonances are broad at room temperature, either their $^{13}\text{C}\{^1\text{H}\}$ NMR or low-temperature ^1H NMR spectra are consistent with the incomplete cubane structure lacking



one vertex, shown in Scheme 1, as substantiated⁷ for $[\text{CpTi}(\mu_3\text{-S})_3\{\text{Rh}(\text{tfbb})\}_3]$ by X-ray diffraction methods. The most relevant feature from the spectroscopic data is that the three diolefin ligands are equivalent, showing only two olefinic proton or carbon signals, as expected for the high symmetry (C_{3v}) of the proposed structures.

The reactions leading to **1** and $[\text{CpTi}(\mu_3\text{-S})_3\{\text{Rh}(\text{tfbb})\}_3]$ from $\text{Cp}_2\text{Ti}(\text{SH})_2$ and the appropriate methoxorhodium complexes proceed through a complicated mechanism sensitive to water⁸ and other nucleophiles such as methanol, which is produced in the reactions. Noteworthy observations on these syntheses are the incorporation of an extra sulfido ligand in the products, the removal of a cyclopentadienyl ligand initially bonded to titanium, and the loss of some titanium from the starting material as unknown cyclopentadienyl products (Scheme 1).

Assuming that the extra sulfido ligand comes from a transfer between two titanium atoms, it would require the intermediacy of a species with sulfido ligands bridging two titanium centers. The formation of such a dinuclear species and the removal of the cyclopentadienyl ligand for these reactions is exemplified in a simple way by the reaction of $\text{Cp}_2\text{Ti}(\text{SH})_2$ with BuLi. For this simplest case, mono-deprotonation of the titanium complex, either with NaH or BuLi, would take place in the first instance to give the undetected intermediate $[\text{Cp}_2\text{Ti}(\text{S})(\text{SH})]^-$,¹¹ followed by a transfer of the proton on the hydrosulfido ligand to one cyclopentadienyl ring. Similarly, it could be proposed that $\text{Cp}_2\text{Ti}(\text{SH})_2$ is deprotonated by $[\{\text{Rh}(\mu\text{-Ome})(\text{cod})\}_2]$ to give methanol and a dinuclear species such as **A**. This unobserved intermediate species would lose a cyclopentadienyl ring, as does the anion $[\text{Cp}_2\text{Ti}(\text{S})(\text{SH})]^-$, either spontaneously or through interaction with methanol. Removal of one Cp ring from the reaction of bis(cyclopentadienyl) titanium complexes with methanol is a well-known

(9) Köpf, H.; Schmidt, M. *Angew. Chem., Int. Ed. Engl.* **1965**, *4*, 953.

(10) Bright, T. A.; Jones, R. A.; Koshmieder, S. U.; Nunn, C. M. *Inorg. Chem.* **1988**, *27*, 3819.

(11) Lundmark, P. J.; Kubas, G. J.; Scott, B. L. *Organometallics* **1996**, *15*, 3631.

feature of this kind of compound.¹² Thus, the intermediate formation of a tetranuclear species such as **B** with four sulfido bridging ligands is possible.

A compound such as **B** is the expected product from the reactions of the anionic complex $[\text{Cp}_2\text{Ti}_2(\mu\text{-S})_2(\text{S})_2]^{2-}$ with the chlorocomplexes $[\{\text{M}(\mu\text{-Cl})(\text{diolofin})\}_2]$. Thus, both synthetic routes would have this common intermediate **B**. A further reaction of this hypothetical compound with $[\{\text{M}(\mu\text{-Cl})(\text{diolofin})\}_2]$ or $[\{\text{M}(\mu\text{-OMe})(\text{diolofin})\}_2]$ would lead to the asymmetrical breaking of the sulfido bridges, rendering the heterotetranuclear complexes $[\text{CpTi}(\mu_3\text{-S})_3\{\text{M}(\text{diolofin})\}_3]$ (**1**, **2**, **3**) along with cyclopentadienyltitanium complexes (not isolated). This simplified mechanism explains the features for both synthetic approaches assuming the simplest intermediates. However, more complicated pathways with higher nuclearity intermediates could also be proposed.

Tetranuclear Titanium–Iridium Carbonyl Complexes and Clusters. Replacement of the diolofin ligands in complexes **1–3** takes place cleanly to give the hexacarbonyl compounds $[\text{CpTi}(\mu_3\text{-S})_3\{\text{M}(\text{CO})_2\}_3]$ (M = Rh,⁷ Ir(**4**)), which are isolated in high yield. Interestingly, the iridium complex **4** is brown-orange in solution but navy-blue in the solid state, probably due to intermolecular metal–metal interactions. The nuclearity and the incomplete cubane framework of the starting materials are maintained in these reactions. Thus, the mass spectrum of **4** shows the molecular ion and the sequential loss of the six carbonyl ligands. Moreover, the proposed C_{3v} symmetry of the molecules is confirmed by a single resonance in the $^{13}\text{C}\{^1\text{H}\}$ NMR spectra for the terminal carbonyl groups and three $\nu(\text{CO})$ bands in the IR spectra.

Reactions of the hexacarbonyl complex **4** with a variety of phosphine and phosphite ligands occur readily with evolution of carbon monoxide to give the complexes $[\text{CpTi}(\mu_3\text{-S})_3\text{Ir}_3(\mu\text{-CO})(\text{CO})_3(\text{PR}_3)_3]$ ($\text{PR}_3 = \text{PPh}_3$ (**5**), PMe_3 (**6**), $\text{P}(\text{OMe})_3$ (**7**), PMePh_2 (**8**)), which are isolated as brown microcrystalline solids in good yield. Complexes **5–8** contain a bridging carbonyl group, as substantiated by a $\nu(\text{CO})$ band in the range 1770–1740 cm^{-1} in the IR spectra. This band is somewhat low in energy for a carbonyl ligand bridging a metal–metal bond and high for a ketonic carbonyl. Characterization of **5–8** relies on elemental analyses and mass spectra, which show the molecular ions and the successive loss of the four CO groups. A unique isomer results from these reactions, since a single Cp resonance is observed in the ^1H NMR spectra. Moreover, since the complexes **5–8** are fluxional, the structure of one representative compound was studied by X-ray diffraction methods (vide infra).

An unexpected result from these types of reactions is the isolation of the complex $[\text{CpTi}(\mu_3\text{-S})_3\{\text{Ir}(\text{CO})(\text{PMe}_2\text{Ph})\}_3]$ (**9**), lacking the bridging carbonyl ligand, from the reaction of **4** with PMe_2Ph . This type of complex is analogous to those resulting from the reactions of monodentate P-donor ligands with the rhodium complex $[\text{CpTi}(\mu_3\text{-S})_3\{\text{Rh}(\text{CO})_2\}_3]$. The structure corresponds to the most symmetrical isomer, since the three phosphine ligands and the three carbonyl groups are equivalent in the $^{31}\text{P}\{^1\text{H}\}$ and $^{13}\text{C}\{^1\text{H}\}$ NMR spectra, respectively.

Additionally, **9** shows a sole broad $\nu(\text{CO})$ band for the three terminal carbonyls. In light of this peculiar result, we attempted to remove one carbonyl group from $[\text{CpTi}(\mu_3\text{-S})_3\text{Ir}_3(\mu\text{-CO})(\text{CO})_3(\text{PR}_3)_3]$ by reaction with trimethylamine *N*-oxide in acetone under reflux, but the starting material was recovered unaltered. In contrast, the decarbonylation of the homologous titanium–rhodium heterotetranuclear complex $[\text{CpTi}(\mu_3\text{-S})_3\text{Rh}_3(\mu\text{-CO})(\text{CO})_3(\text{PPh}_3)_3]$ takes place smoothly. In fact, complex $[\text{CpTi}(\mu_3\text{-S})_3\{\text{Rh}(\text{CO})(\text{PPh}_3)\}_3]$ reacts reversibly with carbon monoxide to give $[\text{CpTi}(\mu_3\text{-S})_3\text{Rh}_3(\mu\text{-CO})(\text{CO})_4(\text{PPh}_3)_2]$ and $[\text{CpTi}(\mu_3\text{-S})_3\text{Rh}_3(\mu\text{-CO})(\text{CO})_3(\text{PPh}_3)_3]$, which are in equilibrium.¹³ Comparing the result of the reactions of $[\text{CpTi}(\mu_3\text{-S})_3\{\text{M}(\text{CO})_2\}_3]$ (M = Rh, Ir(**4**)) with P-donor ligands, the differences between rhodium and iridium can be explained assuming the higher ability of the latter to form metal–metal bonds, but the failure of complex **9** to follow the general trend for the iridium complexes cannot be rationalized in terms of the basicity or the cone angle of the phosphine.

Molecular Structure of $[\text{CpTi}(\mu_3\text{-S})_3\text{Ir}_3(\mu\text{-CO})(\text{CO})_3\{\text{P}(\text{OMe})_3\}_3]$ (7**).** The structural analysis carried out by X-ray diffraction showed the presence of two crystallographically independent—but chemically analogous (see Table 1)—tetranuclear complexes in the solid state. Figure 1 shows a molecular view of one of the independent molecules together with the labeling system used and a conventional representation of the displacement parameters. The heterotetranuclear TiIr_3 framework exhibits an irregular tetrahedral arrangement. Each ideal triangular Ir_2Ti face is capped by a triply bridging sulfide ligand. The titanium center completes a pseudotetrahedral coordination (three-legged piano stool geometry) being η^5 -bonded to a cyclopentadienyl group. On the other hand, each Ir atom is additionally bonded to a terminal carbonyl and a more voluminous $\text{P}(\text{OMe})_3$ ligand. Without considering the Cp and the OMe groups of the phosphite ligands, the symmetry of the whole structure is reduced to C_s by the presence of an additional μ_2 -bridging carbonyl that connects two iridium atoms, Ir(1) and Ir(3). It is worth pointing out the equatorial disposition of all three phosphite ligands relative to the Ir_3 triangle, whereas the four carbonyls adopt *pseudoaxial* positions on the opposite side of the CpTiS_3 moiety (see Figure 1).

As for the closely related rhodium complex $[\text{CpTi}(\mu_3\text{-S})_3\{\text{Rh}(\text{tfbb})\}_3]$,⁷ the central TiIr_3S_3 core exhibits an incomplete cubane-type structure with one vacant site close to the three iridium atoms. However, the internal bond angles in the cubane structure for the iridium compound significantly deviate from the ideal value of 90° (max. dev. 19.6°) and show broader ranges than in the rhodium analogue ($\text{S–Ti–S } 98.5\text{–}109.7(3)^\circ$, $\text{S–Ir–S } 91.9\text{–}103.4(2)^\circ$, $\text{Ti–S–Ir } 72.7\text{–}81.5(2)^\circ$, and $\text{Ir–S–Ir } 70.4\text{–}73.6(2)^\circ$), which reveals the relative reduction of symmetry of the whole molecule. Comparatively, the major difference concerns the M–S–M bond angles, which change from a value of $99.7(1)^\circ$ for the rhodium species to a mean value of $72.1(1)^\circ$ for **7**, reflecting the shorter Ir–Ir separations.

All the geometrical parameters lead to the structural—and consequently electronic—differentiation of two iri-

(12) (a) Höhlein, U.; Schobert, R. *J. Organomet. Chem.* **1992**, *424*, 301. (b) Kalirai, B. S.; Foulon, J. D.; Hamor, T. A.; Jones, C. J.; Beer, P. D. *Polyhedron* **1991**, *10*, 1847.

(13) Casado, M. A.; Pérez-Torrente, J. J.; Ciriano, M. A.; Oro, L. A.; Orejón, A.; Claver, C. *Organometallics* **1999**, *18*, 3035.

Table 1. Selected Bond Distances (Å) and Angles (deg) for Complex 7^a

Ir(1)–Ir(2)	2.9246(14)	2.9087(14)	Ir(3)–Ir(2)	2.9374(14)	2.8912(14)
Ir(1)–Ir(3)	2.8063(14)	2.8131(14)			
Ir(1)⋯Ti	3.112(4)	3.122(4)	Ir(3)⋯Ti	3.127(4)	3.124(4)
Ir(1)–S(1)	2.489(6)	2.502(6)	Ir(3)–S(2)	2.494(7)	2.492(7)
Ir(1)–S(3)	2.442(6)	2.440(6)	Ir(3)–S(3)	2.426(6)	2.442(6)
Ir(1)–P(1)	2.238(7)	2.232(7)	Ir(3)–P(3)	2.237(6)	2.230(7)
Ir(1)–C(101)	1.88(3)	1.84(3)	Ir(3)–C(301)	1.90(2)	1.86(3)
Ir(1)–C(102)	2.07(2)	2.01(3)	Ir(3)–C(102)	2.02(2)	2.04(3)
Ir(2)–Ti	2.806(4)	2.824(4)	Ti–S(1)	2.298(7)	2.297(8)
Ir(2)–S(1)	2.395(6)	2.421(6)	Ti–S(2)	2.321(8)	2.292(7)
Ir(2)–S(2)	2.411(6)	2.417(6)	Ti–S(3)	2.364(8)	2.370(7)
Ir(2)–P(2)	2.200(7)	2.184(6)	Ti–C(10)	2.40(4)	2.37(3)
Ir(2)–C(201)	1.85(3)	1.84(3)	Ti–C(11)	2.40(4)	2.40(3)
C(101)–O(101)	1.14(3)	1.15(3)	Ti–C(12)	2.30(3)	2.32(3)
C(201)–O(201)	1.20(3)	1.17(3)	Ti–C(13)	2.35(3)	2.37(3)
C(301)–O(301)	1.12(3)	1.14(3)	Ti–C(14)	2.38(3)	2.37(3)
C(102)–O(201)	1.15(3)	1.21(3)	Ti–G ^b	2.063(3)	2.067(3)
S(1)–Ir(1)–S(3)	92.5(2)	92.2(2)	S(2)–Ir(3)–S(3)	92.3(2)	91.9(2)
S(1)–Ir(1)–P(1)	110.2(2)	113.3(2)	S(2)–Ir(3)–P(3)	111.5(2)	112.7(2)
S(1)–Ir(1)–C(101)	88.6(8)	86.5(8)	S(2)–Ir(3)–C(301)	90.9(7)	91.4(10)
S(1)–Ir(1)–C(102)	143.2(6)	142.6(8)	S(2)–Ir(3)–C(102)	144.2(6)	142.5(8)
S(3)–Ir(1)–P(1)	90.9(2)	90.6(2)	S(3)–Ir(3)–P(3)	91.7(2)	90.3(2)
S(3)–Ir(1)–C(101)	177.5(8)	177.3(8)	S(3)–Ir(3)–C(301)	172.6(7)	175.7(10)
S(3)–Ir(1)–C(102)	80.7(6)	82.0(8)	S(3)–Ir(3)–C(102)	82.0(6)	81.4(8)
P(1)–Ir(1)–C(101)	90.8(9)	92.1(8)	P(3)–Ir(3)–C(301)	93.4(7)	91.1(9)
P(1)–Ir(1)–C(102)	106.0(6)	103.7(8)	P(3)–Ir(3)–C(102)	104.0(6)	104.3(8)
C(101)–Ir(1)–C(102)	97.1(10)	97.6(11)	C(301)–Ir(3)–C(102)	91.5(9)	94.3(12)
S(1)–Ir(2)–S(2)	103.4(2)	101.7(2)	G ^b –Ti–S(1)	113.9(9)	115.1(9)
S(1)–Ir(2)–P(2)	100.8(2)	101.8(2)	G–Ti–S(2)	117.0(10)	114.7(9)
S(1)–Ir(2)–C(201)	126.6(9)	124.4(8)	G–Ti–S(3)	116.0(10)	116.8(8)
S(2)–Ir(2)–P(2)	96.1(3)	97.6(2)	S(1)–Ti–S(2)	109.5(3)	109.7(3)
S(2)–Ir(2)–C(201)	126.6(8)	131.8(8)	S(1)–Ti–S(3)	99.6(3)	99.5(3)
P(2)–Ir(2)–C(201)	92.3(9)	86.9(8)	S(2)–Ti–S(3)	98.5(3)	99.0(3)
Ir(1)–S(1)–Ti	81.0(2)	81.1(2)	Ir(3)–S(2)–Ti	80.9(2)	81.4(2)
Ir(1)–S(1)–Ir(2)	73.5(2)	72.4(2)	Ir(3)–S(2)–Ir(2)	73.6(2)	72.1(2)
Ir(2)–S(1)–Ti	73.4(2)	73.5(2)	Ir(2)–S(2)–Ti	72.7(2)	73.6(2)
Ir(1)–S(3)–Ti	80.7(2)	80.9(2)	Ir(1)–C(101)–O(101)	176(2)	176(3)
Ir(1)–S(3)–Ir(3)	70.4(2)	70.4(2)	Ir(2)–C(201)–O(201)	176(2)	178(2)
Ir(3)–S(3)–Ti	81.5(2)	80.9(2)	Ir(3)–C(301)–O(301)	175(2)	178(3)
Ir(1)–C(102)–O(102)	135(1)	137(2)	Ir(3)–C(102)–O(102)	138(2)	134(2)
Ir(1)–C(102)–Ir(3)	86.7(8)	87.7(11)			

^a The two values stated for each parameter correspond to the two crystallographically independent molecules. ^b G represents the centroid of the C₅H₅ ring. Mean values over the two independent molecules and over all chemically equivalent bonds have been used in the discussion.

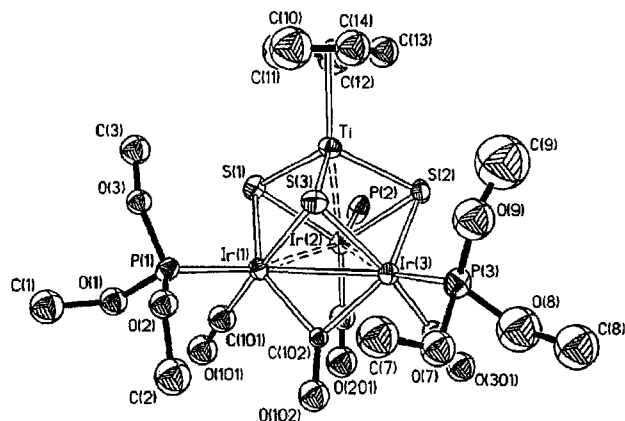


Figure 1. Drawing of the molecular structure of one of the two independent molecules of 7, together with labeling scheme used. Methoxy groups of one phosphite ligand (P(2)) have been omitted for clarity.

dium atoms, Ir(1) and Ir(3), from the third one, Ir(2). Thus, without considering metal–metal interactions, the coordination environment of Ir(1) and Ir(3) could be described as slightly distorted trigonal bipyramid, common for dinuclear iridium(II) complexes, with the axial positions occupied by the atom S(3) and by their respective terminal carbonyls. On the other hand, Ir(2) exhibits an anomalous distorted tetrahedral coordina-

tion; bond angles around Ir(2) are in the range 86.9–131.8(8)°, with a mean value of 107.5(3)°. This coordination geometry is quite uncommon for a formal Ir(I) atom and might be a consequence of the bonding interactions between the metals.

The description of the intermetallic bonding system is subject to interpretation. Concerning the Ir–Ti separations, there are two statistically identical longer distances (mean 3.121(2) Å) and a shorter separation Ir(2)–Ti of 2.815(3) Å. Unfortunately, no previous complex with Ti and Ir metals in close proximity has been structurally characterized.¹⁴ All these distances are significantly longer than metal–metal separations observed for complexes such as [CH₃–C(CH₂NSiMe₃)₃Ti–M(CO)₂Cp] (M = Ru, 2.527(1); Fe, 2.441(5) Å) with a clear unsupported metal–metal bond,¹⁵ for direct Ti–Rh metal–metal bonds found in Ti/Rh alloys, 2.68 Å,¹⁶ and for a triple Ti–Rh bond in the recently reported complex [Ti(*μ*-OCMe₂CH₂PPh₃)₃Rh], 2.2142(11) Å.¹⁷

(14) Allen, F. H.; Kennard, O. *Chem. Des. Automation News* **1993**, 8, 1 and 31.

(15) Friedrich, S.; Memmler, H.; Gade, L. H.; Li, W. S.; McPartlin, M. *Angew. Chem., Int. Ed. Engl.* **1994**, 33, 676. Friedrich, S.; Memmler, H.; Gade, L. H.; Li, W. S.; Scowen, I. J.; McPartlin, M.; Housecroft, C. E. *Inorg. Chem.* **1996**, 35, 2433.

(16) Tauster, S. J. *Acc. Chem. Res.* **1987**, 20, 389. Sakellson, S.; McMillan, M.; Haller, G. L. *J. Phys. Chem.* **1986**, 90, 1733.

However, the Ir(2)–Ti separation is significantly shorter than the values reported for the rhodium analogue $[\text{CpTi}(\mu_3\text{-S})_3\text{Rh}_3(\text{tfbb})_3]$ (2.924(2) Å), where a dative interaction— σ bonding in character—from the electron-rich d^8 metal to the d^0 titanium center has been suggested.⁷ Similar intermetallic separations in the range 2.789(3)–2.986(1) Å have also been observed in dinuclear thiolate¹⁸ or methylene-bridged¹⁹ Rh–Ti complexes or in related Ti–Pt acetylene-bridged species²⁰ and in all these cases have been considered indicative of a dative M–Ti bonding interaction. All these facts seem to support the presence in **7** of a bonding interaction between the tetrahedral Ir(2) atom and the titanium center. On the other hand, the longer Ir–Ti separations determined for the Ir(1) and Ir(3) atoms (3.121 Å) preclude the proposal of any but the weakest Ir–Ti interaction.

Regarding the Ir–Ir separations, the situation is similar to that mentioned for the Ir–Ti distances: there is one short Ir–Ir distance, 2.8097(10) Å, and two slightly longer ones (range 2.8912–2.9374(14) Å), all of them in the range of metal–metal interactions or bonds. The shorter Ir(1)–Ir(3) distance is at the upper end of the range of bond distances observed in related tetranuclear Ir₄ clusters where two or more “Ir(CO)PR₃” moieties are connected by μ_2 -bridging carbonyls; these are the cases of $[\text{Ir}_4(\mu\text{-CO})_3(\text{CO})_5(\text{PMe}_3)_4]$ (2.715–2.794(1) Å),²¹ $[\text{Ir}_4(\mu\text{-CO})_3(\text{CO})_5(\text{PPhMe}_2)_4]$ (2.726–2.782(3)),²² or $[\text{Ir}_4(\mu\text{-CO})_3(\text{CO})_7(\text{PPh}_3)_2]$ (2.767–2.782(2) Å).²³ Similar values have also been reported for related trinuclear $[\text{Ir}_3(\mu\text{-CO})(\mu\text{-S}^t\text{Bu})_3(\text{CO})_4(\text{PMe}_3)_2]$ (2.712(3) Å)²⁴ or binuclear $[\text{Ir}_2(\mu\text{-CO})(\mu\text{-S}^t\text{Bu})(\text{S}^t\text{Bu})(\text{CO})_2(\text{PMe}_3)_3]$ (2.702(1) Å)²⁴ and $[\text{Ir}_2(\mu\text{-CO})(\mu\text{-S})(\mu\text{-dppm})_2(\text{CO})_2]$ (2.843(2) Å)²⁵ complexes with thiolate and carbonyl groups connecting two Ir(I) centers and for which metal–metal Ir–Ir bonds have been established. Moreover, the observation of a $^3J_{\text{P-P}}$ coupling constant in the $^31\text{P}\{^1\text{H}\}$ NMR spectrum of the rhodium analogue of **7**, $[\text{CpTi}(\mu_3\text{-S})\text{Rh}_3(\mu\text{-CO})(\text{CO})_3(\text{PPh}_3)_3]$, provides an additional support for an analogous structure for the rhodium derivative and for the presence of an Ir(1)–Ir(3) metal–metal bond in **7**. The two remaining Ir–Ir separations, Ir(1)–Ir(2) and Ir(3)–Ir(2), are only 0.11 Å longer than that of a carbonyl-bridged metal–metal bond, and consequently, the existence of a metal–metal bonding interaction between these metals is possible.

The Ir–S and the Ir–P bond distances also reflect the different electronic characteristics of the metal centers. Thus, the Ir–S bond distances change gradually from

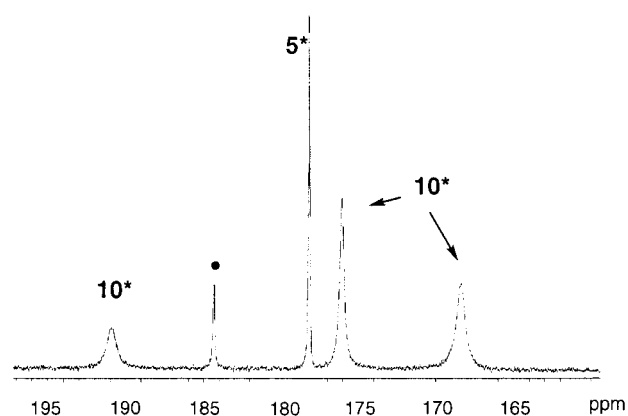


Figure 2. $^{13}\text{C}\{^1\text{H}\}$ NMR spectrum of $[\text{CpTi}(\mu_3\text{-S})_3\text{Ir}_3(\mu\text{-CO})(\text{CO})_3(\text{PPh}_3)_3]$ (**5**) under a ^{13}CO atmosphere in CDCl_3 at 293 K in the carbonyl region containing **5*** and $[\text{CpTi}(\mu_3\text{-S})_3\text{Ir}_3(\mu\text{-}^{13}\text{CO})(^{13}\text{CO})_4(\text{PPh}_3)_2]$ (**10***) (● dissolved ^{13}CO).

Ir(2)–S 2.411(3), passing through Ir(1/3)–S(3) (trans to terminal carbonyl) 2.437(3), to Ir(1/3)–S (trans to bridging carbonyl) 2.494(4) Å. In accord with this, the Ir(2)–P(2) bond length, 2.192(5) Å, is also statistically shorter than the Ir(1/3)–P(1/3) 2.234(4) Å distances. All these differences conform to the C_s symmetry observed for the metal core.

Labeling Experiments with ^{13}CO and Replacement Reactions. A complete replacement of all the carbonyl groups by ^{13}CO in **5** occurs in a few minutes on stirring a solution of this compound under an atmosphere of ^{13}CO . From this solution $[\text{CpTi}(\mu_3\text{-S})_3\text{Ir}_3(\mu\text{-}^{13}\text{CO})(^{13}\text{CO})_3(\text{PPh}_3)_3]$ (**5***) is isolated. Conversely, complex **5** results from **5*** when treated with natural CO for a few minutes. Curiously, most of the metal carbonyl clusters of iridium and osmium resist exchange reactions with ^{13}CO under mild conditions.²⁶

Indeed, the reaction mixture changes from brown to red under an atmosphere of carbon-13 monoxide and contains mainly a new compound, $[\text{CpTi}(\mu_3\text{-S})_3\text{Ir}_3(\mu\text{-}^{13}\text{CO})(^{13}\text{CO})_4(\text{PPh}_3)_2]$ (**10***), along with free PPh_3 and a small amount of complex **5*** (Figure 2). As the atmosphere of carbon monoxide is removed, complex **5*** results. Thus, the equilibrium between **5*** and **10*** is easily shifted in one or the opposite direction depending on the working conditions (Scheme 2). The replacement of phosphine by carbon monoxide does not go further than **10*** at atmospheric pressure. The reverse reaction can be monitored by adding PPh_3 to the complex $[\text{CpTi}(\mu_3\text{-S})_3\text{Ir}_3(^{13}\text{CO})_6]$ (**4***), prepared easily by carbonylation of **3** with ^{13}CO . Addition of 1 molar equiv of PPh_3 to **4*** results in a mixture of the starting material, **10***, and a small amount of a complex assumed to be $[\text{CpTi}(\mu_3\text{-S})_3\text{Ir}_3(\mu\text{-}^{13}\text{CO})(^{13}\text{CO})_5(\text{PPh}_3)]$. The latter complex contains all the carbonyl groups of the starting material and shows a single Cp resonance at δ 5.72 ppm and at δ 105.0 ppm in the ^1H NMR and $^{13}\text{C}\{^1\text{H}\}$ NMR spectra, respectively. The carbonyl groups give rise to a featureless resonance at δ 167.0 ppm, while new terminal and bridging $\nu(^{13}\text{CO})$ carbonyl stretches are observed at 2034, 1994, 1940, and 1751 cm^{-1} . Addition of a second molar equivalent of PPh_3 leads to the replacement of carbonyl ligands to give mainly **10*** along with some of **5***. Further additions of PPh_3 only modify the relative

(17) Slaughter, L. M.; Wolczanski, P. T. *J. Chem. Soc., Chem. Commun.* **1997**, 2109.

(18) Nadasdi, T. T.; Stephan, D. W. *Inorg. Chem.* **1994**, *33*, 1532, and references therein.

(19) Park, J. W.; Henling, L. M.; Schaefer, W. P.; Grubbs, R. H. *Organometallics* **1991**, *10*, 171. Ozawa, F.; Park, J. W.; Mackenzie, P. B.; Schaefer, W. P.; Henling, L. M.; Grubbs, R. H. *J. Am. Chem. Soc.* **1989**, *111*, 1319. Park, J. W.; Mackenzie, P. B.; Schaefer, W. P.; Grubbs, R. H. *J. Am. Chem. Soc.* **1986**, *108*, 6402.

(20) Berenguer, J. R.; Forniés, J.; Lalinde, E.; Martín, A. *Angew. Chem., Int. Ed. Engl.* **1994**, *33*, 2083.

(21) Darenbourg, D. J.; Baldwin-Zuschke, B. J. *Inorg. Chem.* **1981**, *20*, 3846.

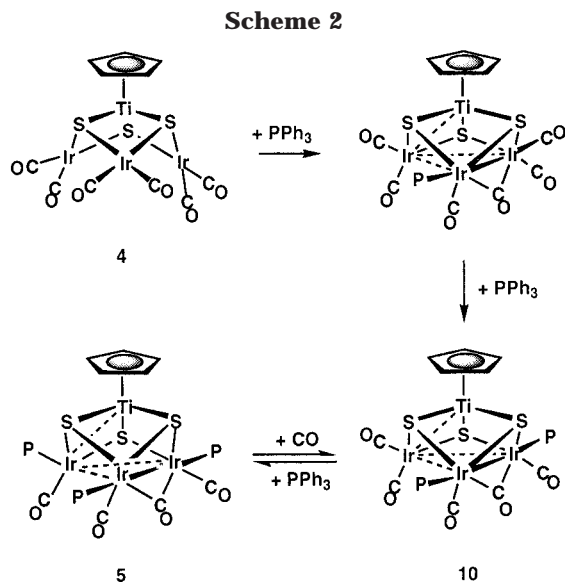
(22) Blake, A. J.; Osborne, A. G. *J. Organomet. Chem.* **1984**, *260*, 227.

(23) Florke, U.; Haupt, H. J. *Z. Kristallogr.* **1990**, *191*, 149.

(24) Kalck, P.; Bonnet, J. J.; Poilblanc, R. *J. Am. Chem. Soc.* **1982**, *104*, 3069.

(25) Kubiak, C. P.; Woodcock, C.; Eisenberg, R. *Inorg. Chem.* **1980**, *19*, 2733.

(26) Ros, R.; Tassan, A. *Inorg. Chim. Acta* **1997**, *260*, 89.



proportions of **5**/**10*** and free phosphine in the equilibrium while the carbon monoxide atmosphere is maintained.

Characterization of complex **10***, which was not isolated, relies on IR and multinuclear NMR spectroscopy. This complex shows singlets at -15.8 and 5.21 (for Cp) ppm in the $^{31}\text{P}\{^1\text{H}\}$ and ^1H NMR spectra, respectively, and three broad signals at δ 190.9, 176.1, and 168.4 ppm of relative intensity 1:2:2 in the $^{13}\text{C}\{^1\text{H}\}$ NMR spectrum for the bridging and four terminal carbonyl groups, respectively (Figure 2), along with a bridging $\nu(^{13}\text{CO})$ stretch at 1720 cm^{-1} . Bearing in mind the structure of **7**, all these data fit with the structure proposed for **10*** in Scheme 2; that is, the triiridium triangle is face-capped by the CpTi(S)₃ moiety. Within the metal triangle an iridium atom, probably in a tetrahedral environment, possesses two terminal carbonyl ligands, while the other two iridium atoms are bonded to two phosphine ligands in the Ir₃ plane and to a bridging and two terminal carbonyls in axial positions. Although the three carbonyl environments are detected for **10***, $^{13}\text{C}-^{31}\text{P}$ couplings are not observed, and no further spectroscopic information is available due to the broadening of the signals.

The replacement equilibrium **5** \rightleftharpoons **10** between the carbonyl and phosphine ligands apparently takes place at the tetrahedral iridium atom. Taking this view only, one would expect that the exchange between CO and labeled ^{13}CO would occur only at this iridium atom, but this is not the case. Therefore a further process ensures the easy exchange of all the carbonyl ligands (vide infra).

Monitoring the reaction of **4*** with PMe_2Ph indicates a pathway in which complexes with bridging carbonyl groups are absent. A replacement of carbonyl groups occurs on addition of 1 molar equiv of PMe_2Ph to **4*** to give a mixture of the final product (**9***) along with the starting material and an intermediate complex thought to be $[\text{CpTi}(\mu_3\text{-S})_3\text{Ir}_3(^{13}\text{CO})_4(\text{PMe}_2\text{Ph})_2]$. This latter complex is fluxional, showing two broad bands for the carbonyl groups around δ 177 and 170 ppm in the $^{13}\text{C}\{^1\text{H}\}$ NMR spectrum and singlets for the Cp group and phosphine ligands at δ 5.50 and -51.9 ppm in the ^1H NMR and $^{31}\text{P}\{^1\text{H}\}$ NMR spectra, respectively. Further addition of phosphine leads to an increase in the

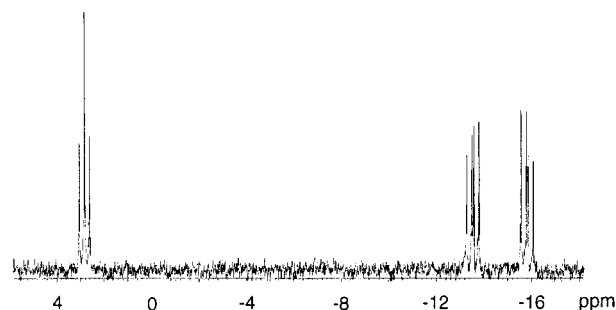


Figure 3. $^{31}\text{P}\{^1\text{H}\}$ NMR spectrum of $[\text{CpTi}(\mu_3\text{-S})_3\text{Ir}_3(\mu\text{-CO})(\text{H})(\text{CO})_3(\text{PPh}_3)_3]\text{BF}_4$ (**11**) in CDCl_3 at 293 K.

quantity of complex **9** isolated. Thus, the main difference between the reactions leading either to **5**–**8** or **9** arises in the first step. For **5**–**8** a movement of a terminal carbonyl to a bridging position accompanies the addition of the phosphine ligand to the starting complex **4**, while for **9** a replacement of one carbonyl ligand follows the incorporation of PMe_2Ph .

Protonation Reaction of $[\text{CpTi}(\mu_3\text{-S})_3\text{Ir}_3(\mu\text{-CO})(\text{CO})_3(\text{PPh}_3)_3]$. The reaction of the complexes $[\text{CpTi}(\mu_3\text{-S})_3\text{Ir}_3(\mu\text{-CO})(\text{CO})_3(\text{PR}_3)_3]$ with the simplest electrophile (H^+) gives insight into the chemical environments of the iridium atoms. In particular, the reaction of $[\text{CpTi}(\mu_3\text{-S})_3\text{Ir}_3(\mu\text{-CO})(\text{CO})_3(\text{PPh}_3)_3]$ (**5**) with 1 molar equiv of HBF_4 is instantaneous and gives a red compound characterized as the monohydrido complex $[\text{CpTi}(\mu_3\text{-S})_3\text{Ir}_3(\mu\text{-CO})(\text{H})(\text{CO})_3(\text{PPh}_3)_3]\text{BF}_4$ (**11**). No further change occurs on addition of an excess of acid. Compound **11** behaves as a 1:1 electrolyte in acetone solution and still contains a bridging carbonyl ligand. This compound is nonfluxional, in contrast with the parent complex **5**, and has no element of symmetry since it shows three inequivalent PPh_3 groups in the $^{31}\text{P}\{^1\text{H}\}$ NMR spectrum (Figure 3). The hydrido ligand is on a single iridium atom and cis to the PPh_3 on this center. This nucleus couples with the three phosphine ligands to give a doublet of triplets in the ^1H NMR spectrum. A selective decoupling $^{31}\text{P}\{^1\text{H}\}$ NMR experiment correlates the main coupling constant to the more deshielded phosphorus resonance. Four carbonyl signals are observed in the $^{13}\text{C}\{^1\text{H}\}$ NMR spectrum; the most deshielded resonance corresponds to the bridging carbonyl, which appears as a multiplet due to the coupling with the three phosphine ligands, while the other three appear as doublets (Figure 4b). These couplings of hydride and the bridging carbonyl with all the phosphorus nuclei are indicative of electronic communication between the atoms of the triiridium triangle probably due to a multicentered metal–metal bonding scheme. A possible structure for **11** fitting all these spectroscopic data is shown in Scheme 3.

The protonation reaction occurs in **5** at the formerly tetrahedral iridium center, which is the most electron-rich metal in the cluster. The stereochemical change of the coordination environment at this atom leads to the loss of the plane of symmetry and, probably, to small changes in the cluster framework. A further indication of electronic communication in the triiridium triangle is that the protonation at an isolated iridium center affects all the iridium atoms in the cluster, as evidenced by the shift of the $\nu(\text{CO})$ bands to higher frequencies relative to **5**.

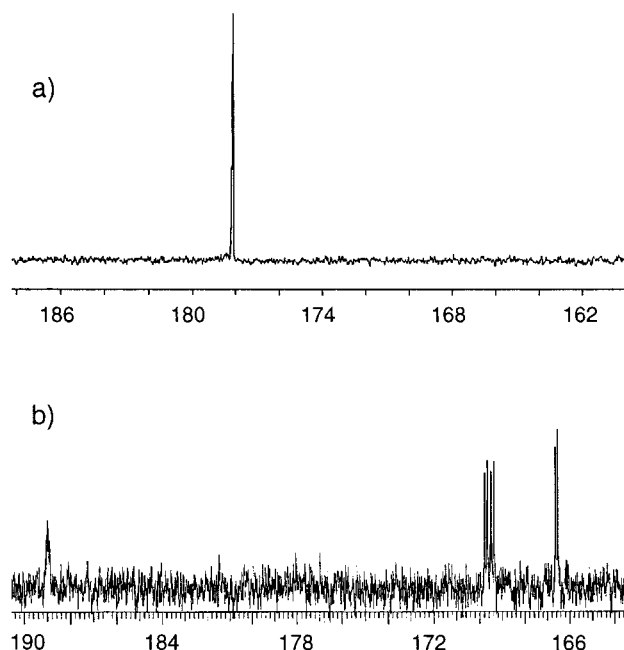
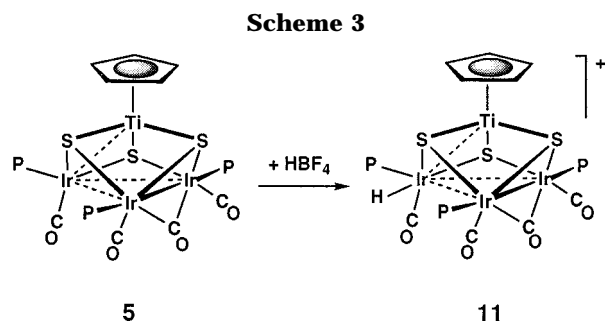
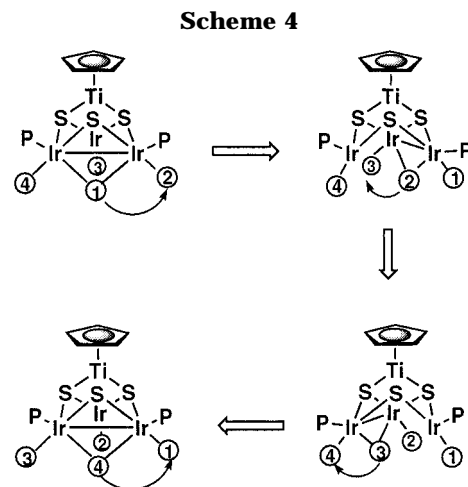


Figure 4. $^{13}\text{C}\{^1\text{H}\}$ NMR spectrum in the carbonyl region of (a) $[\text{CpTi}(\mu_3\text{-S})_3\text{Ir}_3(\mu\text{-CO})(\text{CO})_3(\text{PPh}_3)_3]$ (**5**) in CD_2Cl_2 at 293 K and (b) $[\text{CpTi}(\mu_3\text{-S})_3\text{Ir}_3(\mu\text{-CO})(\text{H})(\text{CO})_3(\text{PPh}_3)_3]\text{BF}_4$ (**11**) in CDCl_3 at 293 K.



Fluxional Behavior and Metal–Metal Bond Mobility. Complexes **5–8** give a single signal for the phosphine ligands and for all the carbonyl groups in the $^{31}\text{P}\{^1\text{H}\}$ NMR and $^{13}\text{C}\{^1\text{H}\}$ NMR spectra (Figure 4a), even at very low temperature (193 K), while three carbonyl and two phosphorus environments would be predicted on the basis of the structure found in the solid state. Therefore, these compounds undergo a low-energy fluxional process which makes the four carbonyl groups and the three P-donor ligands on the triiridium triangle equivalent. As no change is observed from the variable-temperature NMR spectra, the thermodynamic data and exchange rate constants are unavailable, and the proposed mechanism is established on the basis of chemical intuition. Interestingly, the dynamic behavior of the related titanium–rhodium compound $[\text{CpTi}(\mu_3\text{-S})_3\text{Rh}_3(\mu\text{-CO})(\text{CO})_3(\text{PPh}_3)_3]$ is more informative because ^{31}P – ^{103}Rh couplings are observed, and this has been studied by multinuclear NMR spectroscopy. In fact, the exchange mechanism outlined for the rhodium compound is consistent with the proposal for the titanium–iridium complexes.¹³

The failure to observe ^{13}C – ^{31}P couplings for the carbonyl resonance indicates a diminution and averaging of these coupling constants, as a consequence of rapid changes in the environment of the iridium atoms.



It is worth noting that in the solid state all the carbonyl groups are opposite the CpTiS_3 cap and in axial positions on the triiridium triangle. This suggests a facile concerted migration of the carbonyl ligands from the bridge to terminal positions and vice versa,²⁷ as shown in Scheme 4, which leads to the scrambling of all the carbonyl groups. Moreover, the blocking of the movement by protonation of the tetrahedral iridium center is reasonably explained with this model, since the accessibility to coordination positions on this metal is a key factor for the fluxional process. Furthermore, modifying the chemical environment on this distinct metal by replacement of a phosphine ligand by a carbonyl group, as in $[\text{CpTi}(\mu_3\text{-S})_3\text{Ir}_3(\mu\text{-CO})(\text{CO})_4(\text{PPh}_3)_2]$ (**10**), slows down the fluxional process. Finally, the merry-go-round mechanism along with the chemical equilibrium detected for **5/10** is likely responsible for the fast replacement of all the carbonyl groups in **5** by labeled ^{13}C as mentioned above.

Fluxionality in carbonyl clusters is very common, but a distinctive feature of complexes **5–8** is the presence of a short metal–metal bond, just between the iridium atoms supported by the bridging carbonyl and a tetrahedral iridium center in the solid state. As this ligand moves from bridging to terminal positions while an adjacent terminal carbonyl undergoes the opposite movement, the short metal–metal bond and the tetrahedral iridium atom move sequentially along the edges and along the vertexes of the triiridium triangle, respectively. This process of degenerate dynamics is favored by the axial disposition of all carbonyl groups engaged in the process, the lack of steric hindrance, and the close proximity of the three iridium atoms. A kind of metal–metal bond mobility distinct from our case in being associated with oxidation number exchange of the metals has been proposed by Rauchfuss et al.²⁸ for a series of mixed-valence ruthenium and iridium sulfido clusters, but in the examples reported in this paper no change of oxidation state is observed. All the data suggest that the very stable cap “ $\text{CpTi}(\text{S})_3$ ” holds the metal framework in fixed positions and the dynamic behavior is related to the stereochemical change of the

(27) Farrugia, L. J. *J. Chem. Soc., Dalton Trans.* **1997**, 1783.

(28) Houser, E. J.; Rauchfuss, T. B.; Wilson, S. R. *Inorg. Chem.* **1993**, *32*, 4069. Venturelli, A.; Rauchfuss, T. B. *J. Am. Chem. Soc.* **1994**, *116*, 4824. Houser, E. J.; Amarasekera, J.; Rauchfuss, T. B.; Wilson, S. R. *J. Am. Chem. Soc.* **1991**, *113*, 7440. Houser, E. J.; Venturelli, A.; Rauchfuss, T. B.; Wilson, S. R. *Inorg. Chem.* **1995**, *34*, 6402.

coordination environments of the metals involved. Probably, this movement also encompasses a migration of the CpTi fragment around the triiridium triangle so as to be in proximity to the moving tetrahedral center.

General Comments and Bonding Considerations.

The original aim of this research was the controlled synthesis of early–late complexes supported by sulfido ligands. We initially thought that the deprotonation reactions of Cp₂Ti(SH)₂ with diolefin methoxorhodium and -iridium compounds would yield heterotrinary complexes of the type [Cp₂Ti(μ₃-S)₂{M(diolefin)}₂] (M = Rh, Ir) via the metallaligand [Cp₂Ti(S)₂]²⁻. However, they have proved to be rather more complicated than thought.

For rhodium, the first deprotonation reaction leads to the removal of a cyclopentadienyl group on the titanium to yield intermediates which evolve to the isolated products [CpTi(μ₃-S)₃{Rh(diolefin)}₃]. Most probably these intermediates contain two titanium centers bridged by sulfido ligands, which is required to generate subsequently the fragment [CpTi(S)₃]³⁻, containing three sulfido groups. In support of this view, the simple mono-deprotonation of Cp₂Ti(SH)₂ yields the dinuclear titanium complex [Cp₂Ti₂(μ-S)₂(S)₂]²⁻. Moreover, reaction of this dianionic complex with chloro complexes of rhodium and iridium represents a general synthetic path to the complexes [CpTi(μ₃-S)₃{M(diolefin)}₃].

The diolefin complexes have a cap consisting of the early metal [CpTi(S)₃]³⁻ on a trimetal triangle of the late metals. This assembly of the four metals held together by sulfido ligands has an open cubane structure and several unusual features. Thus, the group [CpTi(S)₃]³⁻ has no simple precursors in the chemistry of titanium and in these complexes should be formed and stabilized by coordination to the metals. In fact, this type of early metal sulfide has been described for tantalum,^{29a} and some related cyclopentadienyltitaniumtris(thiolate) complexes are known,^{4a} which have given rise to speculations on the multiple bonding in [CpMS₃]ⁿ⁻ (n = 3, M = Ti; n = 2 M = Ta).^{29b,30} Apart from the MoCo clusters, early–late complexes with sulfido ligands are unusual, as indicated by a recent synthesis of [CpTa(μ-S)₂(S){Rh(cod)}₂].³¹ Moreover, the novel early–late tetrametallic framework is firmly held together by the bridging ligands, as shown by replacement reactions that occur on the late metals, with the diolefin complexes [CpTi(μ-S)₃{M(diolefin)}₃] serving as key compounds in this chemistry.

Reactions of these complexes with carbon monoxide take place on the rhodium and iridium centers, resulting in simple replacement reactions of all the diolefin ligands to produce *cis*-M(CO)₂ groups, as usually occurs for mononuclear complexes. However, further reactions of the carbonyl complexes [CpTi(μ₃-S)₃{M(CO)₂}₃] with phosphorus donor ligands result in the 62-e valence clusters [CpTi(μ₃-S)₃M₃(μ-CO)(CO)₃(PR₃)₃] with a fourth bridging carbonyl ligand. These species are stable and isolated for M = Ir, but they are labile for M = Rh,

releasing carbon monoxide to yield the 60-e valence complexes [CpTi(μ₃-S)₃{Rh(CO)(PR₃)₃}].

An unexpected feature in the structure of the Ti–Ir complex [CpTi(μ₃-S)₃Ir₃(μ-CO)(CO)₃{P(OMe)₃}₃] (**7**) is the presence of one tetrahedral iridium center (if the contacts with the other three metals are ignored). From our point of view, it is quite interesting to note the close relationship between the bonding in the metal framework and the tetrahedral coordination of one iridium center. This unusual coordination stereochemistry for iridium is also shown by dinuclear rhodium(I) and iridium(I) phosphide complexes for which a double M=M bond was proposed.³² Thus, the fragment Ir(CO)(PR₃) should be metal–metal-bonded to the two pentacoordinated iridium atoms, which in turn support a shorter metal–metal bond, through delocalized 3c–4e bonds. In addition, this tetrahedral iridium center shows a close contact with the titanium atom, suggesting at least an electronic communication between these metals.

Considering the intermetallic bonding system from a classical metal cluster approach, complex **7**, and the related **5–8**, are 62-e clusters, and consequently, a metal butterfly framework would be expected.³³ However, the molecular structure found for **7** contains an Ir₃ triangle with three Ir–Ir bonding interactions and only one Ir–Ti metal–metal interaction. The failure to form two Ir–Ti bonds to achieve the butterfly structure (5 M–M bonds), and the relatively elongated metal–metal bonds observed, could probably be understood bearing in mind the electron-poor nature of the titanium center and the weak tendency of the early transition metals to complete their coordination sphere.

The tetrahedral coordination of one iridium atom, together with the equatorial disposition of the phosphite ligands and consequent axial disposition for the carbonyls, and the metal–metal bonding in the triiridium triangle are crucial in explaining the chemical and dynamic behavior of these compounds. Indeed, while the bridging carbonyl group moves along the triangle, all the iridium centers are successively exchanging their stereochemistry, becoming tetrahedral and interacting with the titanium center. Moreover, the carbonyl exchange in these clusters with external CO is very fast for two reasons. First, the tetrahedral iridium offers a coordination site for an entering carbon monoxide to replace one phosphine ligand or vice versa, giving rise to replacement equilibria, as found for [CpTi(μ₃-S)₃M₃(μ-CO)(CO)₃(PPh₃)₃] and [CpTi(μ₃-S)₃M₃(μ-CO)(CO)₄(PPh₃)₂]. Second, once that carbon monoxide becomes coordinated, it moves rapidly from one iridium atom to the next on the trimetal triangle supported by the CpTiS₃ cap, producing the carbonyl scrambling proposed for the dynamic behavior. Furthermore, the vacancy at the tetrahedral iridium is removed by protonation, which also reveals that this is an electron-rich metal

(29) (a) Tatsumi, K.; Inoue, Y.; Nakamura, A. *J. Am. Chem. Soc.* **1989**, *111*, 782. (b) Tatsumi, K.; Kawaguchi, H.; Inoue, Y.; Kohsaka, M.; Nakamura, A.; Cramer, R. E.; VanDoorne, W.; Taogoshi, G. J.; Richmann, P. N. *Organometallics* **1993**, *12*, 352.

(30) Nadasdi, T. T.; Huang, Y.; Stephan, D. W. *Inorg. Chem.* **1993**, *32*, 347.

(31) Tatsumi, K.; Kawaguchi, H.; Inoue, Y.; Nakamura, A.; Cramer, R. E.; Golen, J. A. *Angew. Chem., Int. Ed Engl.* **1993**, *32*, 763.

(32) Arif, A. M.; Heaton, D. E.; Jones, R. A.; Kidd, K. B.; Wright, T. C.; Whittlesey, B. R.; Atwood, J. L.; Hunter, W. E.; Zang, H.-M. *Inorg. Chem.* **1987**, *26*, 4065. Arif, A. M.; Jones, R. A.; Seeberger, M. H.; Whittlesey, B. R.; Wright, T. C. *Inorg. Chem.* **1986**, *25*, 3943. Kang, S. K.; Albright, T. A.; Wright, T. C.; Jones, R. A. *Organometallics* **1985**, *4*, 666.

(33) Mingos, D. M. P. In *The Chemistry of Metal Cluster Complexes*; Shriver, D. F., Kaesz, H. D., Adams, R. D., Eds.; VCH: Weinheim, Germany, 1990; p. 11.

center. Once protonated, the carbonyl scrambling ceases, but communication between the three iridium atoms is still detected through NMR spectroscopy.

Experimental Section

Literature procedures were used to prepare $\text{Cp}_2\text{Ti}(\text{SH})_2$,³⁴ $[\text{M}_2(\mu\text{-Cl})_2(\text{diolefin})_2]$,³⁵ and $[\{\text{M}(\mu\text{-OMe})(\text{cod})\}_2]$.³⁶ All solvents were dried and distilled before use by standard methods, and the new complexes were prepared under an argon atmosphere using Schlenk techniques. Molecular weights were determined with a Knauer osmometer using chloroform solutions. Carbon, hydrogen, and nitrogen analyses were performed in a Perkin-Elmer 2400 microanalyzer. IR spectra were recorded with a Nicolet-IR 550 (4000–400 cm^{-1}) spectrophotometer with the bands calibrated against the sharp peak (1601.4 cm^{-1}) of a polystyrene film. Mass spectra were recorded in a VG Autospec double-focusing mass spectrometer operating in the FAB⁺ mode. ¹H, ¹³C{¹H}, and ³¹P{¹H} spectra were recorded on Varian spectrometers operating at 299.95 and 300.13 MHz for ¹H. Chemical shifts are referenced to SiMe_4 and H_3PO_4 .

[CpTi(μ_3 -S)₃{Rh(cod)}₃] (1). **Method A.** Addition of solid $\text{Cp}_2\text{Ti}(\text{SH})_2$ (0.100 g, 0.413 mmol) to $[\{\text{Rh}(\mu\text{-OMe})(\text{cod})\}_2]$ (0.200 g, 0.413 mmol) in THF (5 mL) gave a red-brown solution from which an orange solid crystallized out for 30 min. This solid was separated by filtration, washed with hexane, and vacuum-dried (0.127 g, 55% yield based on Rh). **Method B:** Butyllithium (1.6 mol·L⁻¹ in hexane, 0.811 mmol) was added to a solution of $\text{Cp}_2\text{Ti}(\text{SH})_2$ (0.198 g, 0.811 mmol) in THF (6 mL) at room temperature to give a green solution for 15 min. Further addition of solid $[\{\text{Rh}(\mu\text{-Cl})(\text{cod})\}_2]$ (0.400 g, 0.811 mmol) gave a brown solution from which an orange solid crystallized for 2 h. The solid was separated as above (0.240 g). The mother liquor was evaporated to dryness and the residue chromatographed on a column of silica gel (2.5 × 10 cm) using 1:1 hexane/dichloromethane as eluent to give an orange band. Evaporation of this solution and addition of hexane rendered an additional crop of orange microcrystals (0.055 g) in 65% combined yield based on Rh. Anal. Calcd for $\text{C}_{29}\text{H}_{41}\text{Rh}_3\text{S}_3\text{Ti}$: C, 41.34; H, 4.90. Found: C, 41.23; H, 4.76. FAB (*m/z*): 842 (M^+ , 87). ¹H RMN (CDCl_3 , rt): δ 5.71 (s, 5H, Cp), 4.84 (br s, 12H, =CH), 2.13 (br s, 24H, CH_2) (cod). ¹³C{¹H} RMN (CDCl_3 , rt): δ 102.9 (s, Cp), 82.2 (br d, =CH), 78.2 (br d, =CH), 31.5 (s, CH_2) (cod).

[CpTi(μ_3 -S)₃{Rh(nbd)}₃] (2). Addition of solid $\text{Cp}_2\text{Ti}(\text{SH})_2$ to a suspension of $[\{\text{Rh}(\mu\text{-OMe})(\text{nbd})\}_2]$ (0.150 g, 0.332 mmol) in toluene (5 mL) gave a red solution from which a yellow microcrystalline solid precipitated for 2 h. This solid was filtered, washed with hexane, and vacuum-dried (0.106 g, 60%). Complex **2** can be alternatively prepared in 60% yield as by method B described above. Anal. Calcd for $\text{C}_{26}\text{H}_{29}\text{Rh}_3\text{S}_3\text{Ti}$: C, 39.31; H, 3.68. Found: C, 39.29; H, 3.57. FAB (*m/z*): 794 (M^+ , 23). ¹H RMN (CDCl_3 , rt): δ 5.55 (s, 5H, Cp), 4.30 (br, 12H, =CH), 3.60 (br, 6H, CH), 1.23 (s, 6H, CH_2) (nbd).

[CpTi(μ_3 -S)₃{Ir(cod)}₃] (3). Addition of butyllithium (1.6 mol·L⁻¹ in hexane, 0.447 mmol) to a solution of $\text{Cp}_2\text{Ti}(\text{SH})_2$ (0.109 g, 0.447 mmol) in THF (6 mL) gave a deep-green solution at room temperature. Further reaction of this solution with solid $[\{\text{Ir}(\mu\text{-Cl})(\text{cod})\}_2]$ (0.300 g, 0.447 mmol) for 2 h gave deep-red microcrystals, which were isolated by filtration, washed with hexane, and dried under vacuum (0.190 g). Column chromatography of the mother liquor as described above for **1** gave a second crop of the red solid (0.025 g). Combined yield: 0.215 g (65% based on Ir). Anal. Calcd for $\text{C}_{29}\text{H}_{41}\text{Ir}_3\text{S}_3\text{Ti}$: C, 31.37; H, 3.72. Found: C, 31.41; H, 3.73. FAB

(*m/z*): 1110 (M^+ , 65). ¹H RMN (CDCl_3 , rt): δ 5.60 (s, 5H, Cp), 4.54 (br s, 6H, =CH), 4.47 (br s, 6H, =CH), 2.05 (br m, 6H, CH_2), 1.83 (br m, 18H, CH_2) (cod). ¹³C{¹H} RMN (CDCl_3 , rt): δ 102.7 (s, Cp), 65.8 (br, =CH), 32.3 (s, CH_2) (cod).

[CpTi(μ_3 -S)₃{Ir(CO)₂]₃] (4). Carbon monoxide was bubbled through a solution of $[\text{CpTi}(\mu_3\text{-S})_3\{\text{Ir}(\text{cod})\}_3]$ (0.080 g, 0.072 mmol) in dichloromethane (5 mL) for 5 min to give a brown-orange solution. The bubbling was continued to concentrate the volume of the solution up to 1 mL, and then hexane (10 mL) was added to crystallize a navy-blue microcrystalline solid. The product was isolated by filtration, washed with cold hexane, and dried under vacuum. Yield: 0.055 g (80%). Anal. Calcd for $\text{C}_{11}\text{H}_5\text{Ir}_3\text{O}_6\text{S}_3\text{Ti}$: C, 13.85; H, 0.53. Found: C, 13.85; H, 0.51. FAB⁺ (*m/z*): 954 (M^+ , 15), 927 ($\text{M}^+ - \text{CO}$, 10), 898 ($\text{M}^+ - 2\text{CO}$, 12), 870 ($\text{M}^+ - 3\text{CO}$, 10), 842 ($\text{M}^+ - 4\text{CO}$, 5), 814 ($\text{M}^+ - 5\text{CO}$, 8), 784 ($\text{M}^+ - 6\text{CO}$, 7). IR (CH_2Cl_2 , cm^{-1}): ν (CO), 2087 (vs), 2054 (vs), 2015 (vs). ¹H RMN (CD_2Cl_2 , rt): δ 6.26 (s, Cp). ¹³C{¹H} RMN (CD_2Cl_2 , rt): δ 171.5 (s, CO), 107.5 (s, Cp).

[CpTi(μ_3 -S)₃{Ir(¹³CO)₂]₃] (4*). A suspension of $[\text{CpTi}(\mu_3\text{-S})_3\{\text{Ir}(\text{cod})\}_3]$ (**3**) (0.100 g, 0.090 mmol) in hexane (5 mL) was stirred under an atmosphere of labeled carbon-13 monoxide (¹³CO, 99%) for 30 min. The suspension changed from red to dark-blue. The solid was filtered, washed with cold hexane, and vacuum-dried. Yield: 0.075 g (87%). Anal. Calcd for $\text{C}_{11}\text{H}_5\text{Ir}_3\text{O}_6\text{S}_3\text{Ti}$ (%): C, 14.96; H, 0.53. Found: C, 14.85; H, 0.49. IR (CH_2Cl_2 , cm^{-1}): ν (CO), 2037 (vs), 2008 (vs), 1967 (vs). ¹H RMN (CDCl_3 , rt): δ 6.21 (s, Cp). ¹³C{¹H} RMN (CDCl_3 , rt): δ 170.8 (s, CO), 106.9 (s, Cp).

Preparation of [CpTi(μ_3 -S)₃Ir₃(μ -CO)(CO)₃(PR₃)₃] (5–8). Addition of a solution of the appropriate phosphine or phosphite in dichloromethane (5 mL) to a solution of $[\text{CpTi}(\mu_3\text{-S})_3\{\text{Ir}(\text{CO})_2\}_3]$ (**4**) in dichloromethane (10 mL) gives brown solutions under evolution of carbon monoxide. The solutions were concentrated under vacuum up to 1 mL, and further addition of hexane rendered the products as brown microcrystalline solids, which were filtered, washed with hexane, and vacuum-dried.

[CpTi(μ_3 -S)₃Ir₃(μ -CO)(CO)₃(PPh₃)₃] (5). **5** resulted from reaction of $[\text{CpTi}(\mu_3\text{-S})_3\{\text{Ir}(\text{CO})_2\}_3]$ (0.042 g, 0.044 mmol) and PPh₃ (0.035 g, 0.132 mmol). Yield: 0.068 g (92%). Anal. Calcd for $\text{C}_{63}\text{H}_{50}\text{Ir}_3\text{O}_4\text{P}_3\text{S}_3\text{Ti}$: C, 44.93; H, 2.99. Found: C, 44.91; H, 2.75. MS (FAB⁺, *m/z*): 1684 (M^+ , 30). IR (CH_2Cl_2 , cm^{-1}) ν (CO), 2021 (vs), 2006 (s), 1902 (s), 1747 (s). ¹H RMN (CDCl_3 , rt): δ 7.56 (m, 18H, PPh₃), 7.30 (m, 27H, PPh₃), 4.76 (s, 5H, Cp). ³¹P{¹H} RMN (CDCl_3 , rt): δ 0.7 (s). ¹³C{¹H} RMN (CD_2Cl_2 , 209 K): δ 179.5 (s, CO), 134.3 (d, $J_{\text{P-C}} = 58$ Hz, C_{ipso}), 133.9 (m, C_o), 130.2 (s, C_p), 127.6 (m, C_m) (PPh₃), 103.3 (Cp).

[CpTi(μ_3 -S)₃Ir₃(μ -CO)(CO)₃(PMe₃)₃] (6). **6** resulted from reaction of $[\text{CpTi}(\mu_3\text{-S})_3\{\text{Ir}(\text{CO})_2\}_3]$ (0.091 g, 0.095 mmol) and PMe₃ (0.030 mL, 0.286 mmol). Yield: 0.088 g (82%). This compound is air-sensitive. Anal. Calcd for $\text{C}_{18}\text{H}_{32}\text{Ir}_3\text{O}_4\text{P}_3\text{S}_3\text{Ti}$: C, 19.20; H, 2.86. Found: C, 19.11; H, 2.79. MS (FAB⁺, *m/z*): 1098 ($\text{M}^+ - \text{CO}$, 35). IR (CH_2Cl_2 , cm^{-1}) ν (CO), 2010 (vs), 1990 (vs), 1960 (w), 1940 (w), 1888 (s), 1747 (s). ¹H RMN (CDCl_3 , rt): δ 5.86 (s, 5H, Cp), 1.75–1.72 (m, 27H, CH_3). ³¹P{¹H} RMN (CDCl_3 , rt): δ -46.8 (s). ¹³C{¹H} RMN (CDCl_3 , rt): δ 180.2 (s, CO), 103.5 (s, Cp), 22.0 (d, $J_{\text{P-C}} = 38$ Hz, CH_3).

[CpTi(μ_3 -S)₃Ir₃(μ -CO)(CO)₃(P(OMe)₃)₃] (7). **7** resulted from reaction of $[\text{CpTi}(\mu_3\text{-S})_3\{\text{Ir}(\text{CO})_2\}_3]$ (0.050 g, 0.052 mmol) and P(OMe)₃ (19 mL, 0.157 mmol). Yield: 0.056 g (84%). Anal. Calcd for $\text{C}_{18}\text{H}_{32}\text{Ir}_3\text{O}_{13}\text{P}_3\text{S}_3\text{Ti}$: C, 17.02; H, 2.54. Found: C, 16.98; H, 2.50. MS (FAB⁺, *m/z*): 1270 (M^+ , 100). IR (CH_2Cl_2 , cm^{-1}) ν (CO), 2048 (vs), 2040 (vs), 2019 (vs), 1973 (s), 1917 (s), 1765 (s). ¹H RMN (CDCl_3 , rt): δ 5.80 (s, 5H, Cp), 3.63, 3.61, 3.59 (s, 27H, OCH₃). ³¹P{¹H} RMN (CDCl_3 , rt): δ 88.1 (s). ¹³C{¹H} RMN (CDCl_3 , rt): δ 177.0 (s, CO), 104.2 (s, Cp), 53.2 (s, OCH₃).

[CpTi(μ_3 -S)₃Ir₃(μ -CO)(CO)₃(PMePh₂)₃] (8). **8** resulted from reaction of $[\text{CpTi}(\mu_3\text{-S})_3\{\text{Ir}(\text{CO})_2\}_3]$ (0.100 g, 0.105 mmol) and PMePh₂ (59 mL, 0.315 mmol). Yield: 0.134 g (85%). Anal. Calcd for $\text{C}_{48}\text{H}_{44}\text{Ir}_3\text{O}_4\text{P}_3\text{S}_3\text{Ti}$: C, 38.47; H, 2.96. Found: C,

(34) Shaver, A.; Marmolejo, G.; McCall, J. M. *Inorg. Synth.* **1990**, 27, 65.

(35) Giordano, G.; Crabtree, R. H. *Inorg. Synth.* **1990**, 28, 88. Herde, J. L.; Lambert, J. C.; Senoff, C. V. *Inorg. Synth.* **1974**, 15, 18.

(36) Usón, R.; Oro, L. A.; Cabeza, J. A. *Inorg. Synth.* **1985**, 23, 126.

Table 2. Crystal Data and Data Collection and Refinement for Complex 7

chem formula	C ₁₈ H ₃₂ Ir ₃ O ₁₃ P ₃ S ₃ Ti
fw	1270.03
crystal size, mm	0.32 × 0.31 × 0.24
space group	<i>P</i> 2 ₁ / <i>c</i> (No. 14)
<i>a</i> , Å	10.1800(10)
<i>b</i> , Å	25.012(4)
<i>c</i> , Å	26.110(5)
β, deg	95.510(10)
<i>V</i> , Å ³	6617.5(2)
<i>Z</i>	8
<i>D</i> _{calcd} , g cm ⁻³	2.550
<i>μ</i> , mm ⁻¹	12.650
no. of measd reflns	14009 (2θ ≤ 50°)
no. of unique reflns	11283 (<i>R</i> _{int} = 0.0911)
min, max trasm fact ^a	0.103, 0.191
no. data/restraints/params	11279/0/441
<i>R</i> (<i>F</i>) (<i>F</i> ² ≥ 2σ(<i>F</i> ²)) ^b	0.0655
<i>wR</i> (<i>F</i> ²) (all data) ^c	0.1476

^a An semiempirical ψ -scan absorption correction was applied.

^b $R(F) = \sum |F_o| - |F_c| / \sum |F_o|$ for 6246 observed reflections. ^c $wR(F^2) = [\sum [w(F_o^2 - F_c^2)^2] / \sum [w(F_o^2)^2]]^{1/2}$; $w^{-1} = [\sigma^2(F_o^2) + (0.0593P)^2]$, where $P = [\max(F_o^2, 0) + 2F_c^2]/3$.

38.39; H, 2.82. MS (FAB⁺, *m/z*): 1498 (M⁺, 40), 1470 (M⁺ - CO, 100). IR (CH₂Cl₂, cm⁻¹) ν (CO), 2011 (vs), 1963 (s), 1891 (s), 1775 (w). ¹H RMN (CDCl₃, rt): δ 7.60–7.56 (m, 12H, Ph), 7.40–7.30 (m, 18H, Ph), 5.10 (s, 5H, Cp), 2.25–2.22 (m, 9H, CH₃). ³¹P{¹H} RMN (CDCl₃, rt): δ -15.8 (s).

[CpTi(μ_3 -S)₃{Ir(CO)(PMe₂Ph)}₃] (9). **9** resulted from reaction of [CpTi(μ -S)₃{Ir(CO)₂}₃] (0.100 g, 0.105 mmol) and PMe₂-Ph (21 μ L, 0.157 mmol). Yield: 0.114 g (85%). Anal. Calcd for C₃₂H₃₈Ir₃O₃P₃S₃Ti: C, 29.93; H, 2.98. Found: C, 29.85; H, 2.84. MS (FAB⁺, *m/z*): 1285 (M⁺, 75), 1256 (M⁺ - CO, 100). IR (CH₂-Cl₂, cm⁻¹): ν (CO), 2010 (vs). ¹H RMN (CDCl₃, rt): δ 7.56 (m, 6H, Ph), 7.38–7.28 (m, 9H, Ph), 5.21 (s, 5H, Cp), 1.93 (m, 18H, CH₃). ³¹P{¹H} RMN (CDCl₃, rt): δ -34.4 (s). ¹³C{¹H} RMN (CDCl₃, rt): δ 180.1 (s, CO), 103.5 (Cp), 128–132 (m, PPh), 19.8 (d, *J*_{P-C} = 31 Hz, Me), 18.2 (d, *J*_{P-C} = 30 Hz).

The ¹³CO-labeled compounds **5***, **6***, and **9*** were prepared by an identical procedure starting from [CpTi(μ_3 -S)₃{Ir(¹³-CO)₂}₃] (**4***) and isolated with similar yields. ¹H, ³¹P{¹H}, and ¹³C{¹H} NMR spectra are as described for the unlabeled complexes.

[CpTi(μ_3 -S)₃Ir₃(μ -¹³CO)(¹³CO)₃(PPh₃)₃] (5*) IR (CH₂Cl₂, cm⁻¹): ν (¹³CO), 1973 (vs), 1958 (s), 1855 (s), 1709 (s). [CpTi(μ_3 -S)₃-Ir₃(μ -¹³CO)(¹³CO)₃(PMe₃)₃] (**6***) IR (CH₂Cl₂, cm⁻¹): ν (CO), 1972 (vs), 1953 (vs), 1900 (w), 1843 (s), 1707 (s). [CpTi(μ_3 -S)₃{Ir(CO)(PMe₂Ph)}₃] (**9***) IR (CH₂Cl₂, cm⁻¹): ν (CO), 1973 (vs).

[CpTi(μ_3 -S)₃Ir₃(μ -CO)(H)(CO)₃(PPh₃)₃][BF₄] (11). Addition of HBF₄ (0.059 mmol) in diethyl ether to [CpTi(μ_3 -S)₃Ir₃(μ -CO)(CO)₃(PPh₃)₃] (**5**) (0.100 g, 0.059 mmol) in THF (10 mL) gave a red solution immediately. Evaporation of the solvent under vacuum up to 1 mL and further addition of diethyl ether (10 mL) rendered **11** as a red solid, which was filtered, washed with diethyl ether, and dried under vacuum. Yield: 0.090 g (86%). Anal. Calcd for C₆₃H₅₁BF₄Ir₃O₄P₃S₃Ti: C, 42.69; H, 2.90. Found: C, 42.54; H, 2.75. MS (FAB⁺, *m/z*): 1286 (M⁺, 30). IR (CH₂Cl₂, cm⁻¹): ν (CO), 2054 (vs), 2025 (s), 1778 (s). ¹H NMR (CDCl₃, rt): δ 7.33–7.50 (m, 45H, PPh₃), 4.57 (s, 5H, Cp), -11.32 (dt, *J*_{H-P} = 17.6 Hz, *J*_{H-P} = 1 Hz, 1H, H-Ir). ³¹P{¹H} NMR (CDCl₃, rt): δ 2.8 (t, *J*_{P-P} = 26 Hz), -13.6 (dd, *J*_{P-P} =

36 Hz, *J*_{P-P} = 26 Hz), -15.8 (dd, *J*_{P-P} = 36 Hz, *J*_{P-P} = 26 Hz). ¹³C{¹H} NMR (CDCl₃, rt): δ 189.0 (m, μ -CO), 169.7 (d, *J*_{C-P} = 9 Hz, CO), 169.4 (d, *J*_{C-P} = 11 Hz, CO), 166.5 (d, *J*_{C-P} = 9 Hz, CO), 134.1–133.4 (m, PPh₃), 132.7–131.5 (m, PPh₃), 128.9–128.6 (m, PPh₃), 105.6 (s, Cp). Λ_m (S·cm²·mol⁻¹): 162 (acetone, 4.96 × 10⁻⁴ M).

Crystal Structure Determination of Complex 7. A summary of crystal data, intensity collection, and refinement parameters is reported in Table 2. The brown crystals used for the X-ray analysis were glued to a glass fiber, mounted on a Siemens-P4 diffractometer, and irradiated with graphite-monochromated Mo K α radiation (λ = 0.71073 Å). Cell constants were obtained from the least-squares fit on the setting angles of 25 reflections (10° ≤ 2θ ≤ 18°). A complete set of independent reflections with 2θ up to 50° (-1 ≤ *h* ≤ 11, -1 ≤ *k* ≤ 29, and -31 ≤ *l* ≤ 31) were measured at 153(1) K using the $\omega/2\theta$ scan technique and subsequently corrected for Lorentz and polarization effects. Reflections were also corrected for absorption by a semiempirical method (ψ -scan).³⁷ Three standard reflections were monitored every 100 measurements throughout data collection as a check on crystal and instrument stability; no decay was observed.

The structure was solved by Patterson and subsequent difference Fourier techniques (SHELXTL-PLUS)³⁸ and refined by full-matrix least-squares on *F*² (SHELXL-97).³⁹ Two crystallographically independent molecules were observed. For some oxygens of the methoxy groups a model of disorder could be established (O(5), O(7), and O(9)). They were modeled with two positions with complementary occupancy factors. Anisotropic thermal parameters were used for the heavier atoms of the central skeleton: Ir, Ti, S, and P. All hydrogen atoms were placed at their calculated positions and were refined with positional and thermal riding parameters. The function minimized was $\sum [w(F_o^2 - F_c^2)^2]$. The calculated weighting scheme was $1/[\sigma^2(F_o^2) + (0.0593P)^2]$, where $P = [\max(F_o^2, 0) + 2F_c^2]/3$. All the refinements converged to reasonable *R* factors (Table 2). The highest residual electron density peaks, weaker than 1.81 e/Å³, were situated in close proximity to the disordered atoms or to the metal centers and have no chemical sense. Scattering factors were used as implemented in the refinement program.³⁹

Acknowledgment. We wish to thank Dirección General de Enseñanza Superior (DGES) for financial support (Projects PB95-221-C1 and PB94-1186), the EU Human Capital and Mobility Program, and Diputación General de Aragón for fellowships (to A.J.E. and M.A.C., respectively).

Supporting Information Available: Full listings of crystallographic data, complete atomic coordinates, isotropic and anisotropic thermal parameters, and bond distances and angles for complex **7** (CIF format). This material is available free of charge via the Internet at <http://pubs.acs.org>.

OM990154R

(37) North, A. C. T.; Phillips, D. C.; Mathews, F. S. *Acta Crystallogr.* **1968**, *A24*, 351.

(38) Sheldrick, G. M. *SHELXTL-PLUS*; Siemens Analytical X-ray Instruments: Madison, WI, 1990.

(39) Sheldrick, G. M. *SHELXL-97*, Program for Crystal Structure Refinement; University of Göttingen: Göttingen, Germany, 1997.